ISSN 2278-3091
Volume 9, No.1.5, 2020
International Journal of Advanced Trends in Computer Science and Engineering
Available Online at http://www.warse.org/IJATCSE/static/pdf/file/ijatcse3291.52020.pdf
https://doi.org/10.30534/ijatcse/2020/3291.52020

Ground Penetrating Radar Analysis for Detecting Void in Concrete

Teddy Andriawan[1], A. A. Pramudita[2], Erfansyah Ali[3]
[1]Department of Telecommunication Engineering Telkom University, Bandung, Indonesia, teddyandriawan@student.telkomuniversity.ac.id
[2]Department of Telecommunication Engineering Telkom University, Bandung, Indonesia, pramuditaadya@telkomuniversity.ac.id
[3]Department of Telecommunication Engineering Telkom University, Bandung, Indonesia, erfansyahali@telkomuniversity.ac.id

ABSTRACT

Currently, most of roads layed on concrete as construction base. But there is still much concrete which has damage or disability, one of which is voids. Voids are damage to the concrete in the form of a fairly deep hole. These voids if left unchecked will undermine structural concrete and will lead to other damage such as corrosion of iron contained in the concrete foundation. Voids occur on the inside of the concrete that is not easily detected. Ground Penetrating Radar (GPR) is a radar system which has capability to detect objects below the surface of the ground. GPRMax is a simulation software that has capability to modelling GPR system which the soil medium can be replace to concrete by changing it to different relative permittivity value. In this research, tests were carried out to detect voids in concrete utilizing simulations using GPRMax software. The results of this study produce an analysis of the signal reconstruction in the simulation that is the identification of the signal produced in the A-Scan process and identification of the depth level and position of voids for the B-Scan.

Key words : Ground Penetrating Radar (GPR), voids, GPRMax, concrete, relative permittivity, signal reconstruction.

1. INTRODUCTION

Concrete has a considerable influence on development (construction) throughout the world, including in Indonesia [1]. From the statement of Y. F. Kandi, it can be concluded that the development progress in Indonesia is growing rapidly from year to year. Therefore it is necessary to check the quality of concrete to support the success of the project. Checking the quality of concrete is done because not all concrete prints are printed perfectly, there are still some concrete is not printed perfectly.

If in a project using concrete that is not formed perfectly, it will endanger the building and all parties involved in the project [2]. Checks carried out in the form of visual investigation to identify damage to concrete, especially voids so that the damage can be repaired immediately. Because the damage inside the concrete cannot be seen clearly, we need a media or a method to help check. Void inspect for large area is a problem that causes the utilization of GPR with the result that the detection is more efficient.

At the beginning of the establishment of the GPR, and this method can accurately find metals and non-metals that are in the soil. Apart from being applied in the field of natural geological materials, this method has now been applied to other media such as wood, concrete and asphalt. The same methodology can be applied and is non-destructive, such as testing a concrete structure, the application of the depth scale of the object to be measured varies from centimeters to kilometers[3]. The most common form of GPR measurement is the presence of a transmitter and receiver that is moved above the surface of the object to be tested to detect signal reflections from the subsurface features of the test object[4].

In this research, testing and analysis of voids on concrete using GPRMax based on the reconstruction of generated signal, a medium is modeled to a concrete containing voids, detect damage inside the concrete can not be seen with the eye. The advantage of GPRMax is that it has the same function as the Ground Penetrating Radar (GPR) performance that can measure the depth and position of voids on the test object based on time travel and the samples produced in the reconstruction of the B-Scan signal.

2. GROUND PENETRATING RADAR

GPR also referred to as ground radar, this method displays the appearance of underground structures with high resolution. The principle of GPR is that it emits electromagnetic waves generated by the transmitter antenna[5]. The amplitude and depth depend on the electrical properties of rocks or media and frequency antennas are used. The GPR method can be classified as easy to do so it is suitable for detecting surface structures because this method is non-destructive and the application process is relatively easy and has a high level of accuracy [6].

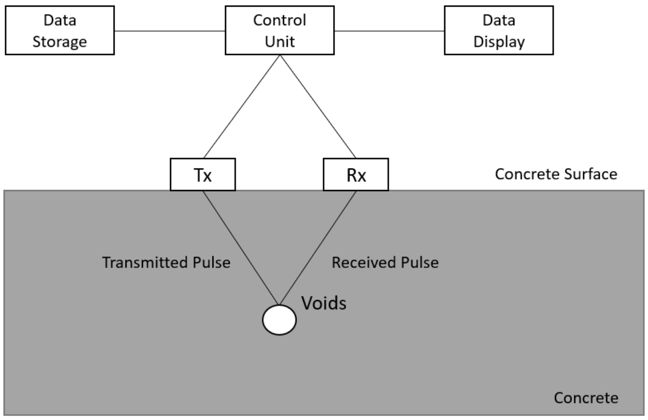

Figure 1: GPR System.

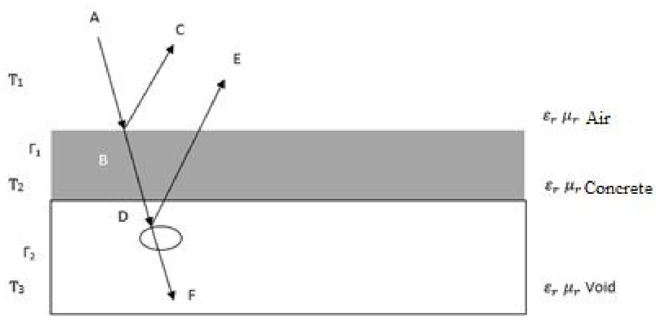

Figure 2: Reflection of Electromagnetic Waves on a Medium.

In Figure 1 explains the GPR system used to detect consists of a control unit, sending and receiving antennas, display equipment, and appropriate data storage. Control unit functions to manage data collection [7]. Transmitter antenna produces electromagnetic waves and sends them to the media to be tested. Receiver antenna converts the received signal into an integer value. Function of receiver antenna to receive pulses that are not absorbed by the earth reflected in the time domain [8].

Figure 2 tells electromagnetic waves that are emitted (A) in concrete has two moments where the wave is transmitted (B) and reflected (C) caused by the presence of two different media (air and concrete) and relative permittivity (ε_r) values. The transmitted electromagnetic wave (D) leads to void, when the wave on voids changes in the medium (concrete and void) and the relative permittivity value (ε_r) resulting in the reflection of the wave (E) and the presence of the transmitted wave (F)[9].

The depth of an object can be measured between time intervals, and transmitting, and receiving pulses. In this time interval, pulses go back and forth from the transmitter antenna to the object and back to the receiver antenna. If t is the time interval, and v is the propagation speed of electromagnetic waves in the ground, then h is stated the depth of the object is as shown in equations 1 and 2[7]:

$$h = {}^{t.v}/_{2} \qquad (1)$$

The speed of electromagnetic waves in the medium of the equation is[7]:

$$v_m = \frac{c}{\sqrt{\varepsilon_r}} \qquad (2)$$

Where v_m= velocity of electromagnetics waves,c = speed of light (3x10^8 m/s), and then ε_r= relative permittivity.

3. FINITE DIFFERENCE TIME DOMAIN (FDTD)

FDTD is a numerical method introduced by K Yee to provide Maxwell's discrete distribution solution. Discretization in the FDTD model is a collection of lattices that are arranged in three dimensions[10]. The forward nature of the GPR classifies it as an initial value - an open boundary issue. This is what is meant by getting a solution that must be set at the start, exciting the GPR transmitter antenna and allowing the resulting field to expand through space to reach zero at infinity because, there are no specific limits that address the geometry of the problem and where the electromagnetic field can take the value which has been specified . Although the first part is easy to accommodate, the second part cannot be easily arranged using limited computing space.

The FDTD approach to the numerical solution of Maxwell's equations is to continuously discretize space and time. So the discretization steps Δx, Δy and Δz play a very significant role, because the smaller they get the closer the FDTD model is to the real representation of the problem. One important parameter when designing GPRMax is determining the discretization step. In the rule of thumb, the discretization step is at least ten times smaller than the smallest wavelength of the propagating electromagnetic field. Wavelength (λ) obtained by equation with[11]:

$$\lambda = \frac{c}{f_m \cdot \sqrt{\varepsilon_r}} \qquad (3)$$

Where λ= waves length (m),c = speed of light (3x10^8 m/s), f_m = frequency maximum and then ε_r= relative permittivity.

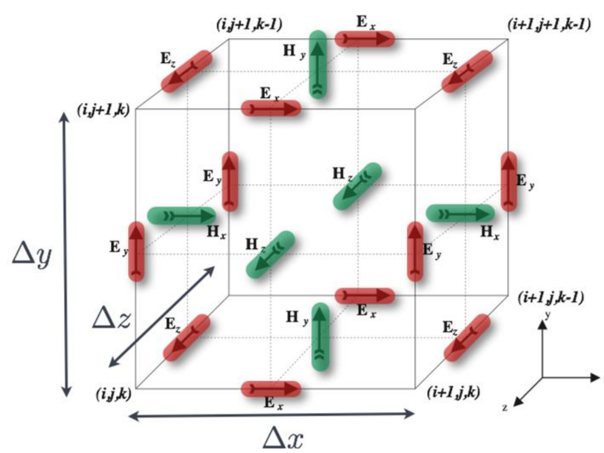

Figure 3: Sigle FDTD Yee Cell Shows Magnetic Field (Green) and Electric Field (Red).

Basically the FDTD method is used to renew the magnetic field and electric field alternately as shown in Figure3. Therefore, there is a timestep, and a grid in this method. In each grid, there are magnetic fields and electric fields in space and time that are updated according to the desired number of timesteps. Some disadvantages of the FDTD method are the computation method, which requires a high memory capacity to perform calculations. FDTD method that uses Cartesian coordinates will give less accurate results, so it requires special treatment. Among several coordinate systems, the Cartesian coordinate system is a coordinate system that is quite simple and is often used. In the Cartesian coordinate system, the grid sizes on all axes, x,*y*, and *z* are homogeneous[12].

GPRMax Simulator is a software that simulates the propagation of electromagnetic waves. This simulator is made by A Giannopoulos based on the method *finite difference time domain* (FDTD) [13].

4. SIMULATION SCENARIOS

For simulation, there are two types of simulation, namely A-Scan and B-Scan simulation. Identify the A-Scan and B-Scan signal with different coordinates of the object position as shown in Table 1 and 2. Signal is obtained from the simulation results using GPRMax by entering the desired parameters as shown in Table 3 and 4, for the A-Scan signal simulation scenario there are 3 conditions. The media used in this simulation is to use concrete by equating the dielectric constant of the measurement media with concrete. Voids modeling in the form of balls with vacuum characteristics.

Table 1: Scenario of A-Scan Simulation.

Number of Object	Coordinate of Object
1 *voids*	10,15,50 (x, y, z)
	20,15,50 (x, y, z)
	30,15,50 (x, y, z)

B-Scan signal is a refinement or reconstruction of the A-Scan signal.

Table 2: Scenario of B-Scan Simulation.

Number of Object	Coordinate of Object
1 void	60, 15, 50 (x, y, z)
2 voids	40, 15, 50 (x, y, z)
	60, 15, 50 (x, y, z)
2 voids	30, 15, 50 (x, y, z)
	60, 15, 50 (x, y, z)

Table 3: Parameters Regulated in A-Scan Research.

Concrete Length	1 m
Concrete Width	1 m
Concrete Hugh	30 cm
Time Window	15 ns
Wave Type	Ricker
Amplitude	1
Frequency	550 MHz
Tx Antenna Position	10, 15, 50 (x, y, z)
Rx Antenna Position	30, 15, 50 (x, y, z)

Table 4: Parameters Regulated in B-Scan Research.

Concrete Length	1 m
Concrete Width	1 m
Concrete High	30 cm
Time Window	15 ns
Wave Type	Ricker
Amplitude	1
Frequency	550 MHz
Tx Antenna Position	10, 15, 50 (x, y, z)
Rx Antenna Position	30, 15, 50 (x, y, z)
Number of Sample	100
Tx and *Rx* Antennas Transition	1 cm

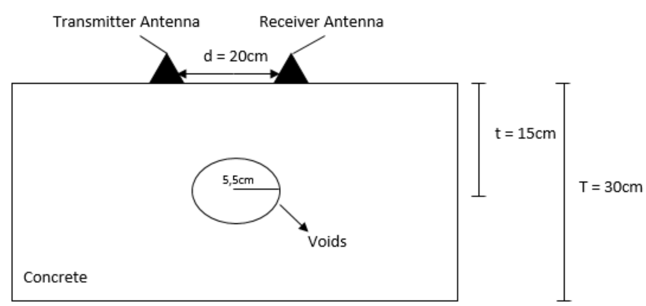

Figure 4: Scenario Simulation.

The simulation scenario uses objects that resemble a voids with a radius 5.5cm, depth of objects are 15cm. Distance of transmitter and receiver antennas are 20 cm, heigh of antennas are 30cm as shown in Figure 4.

5. RESULT & ANALYSIS

5.1 A-Scan Signal Simulation

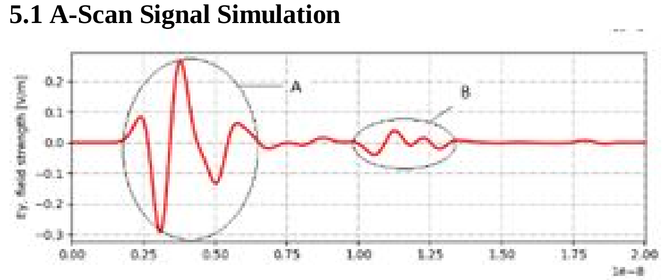

(a)

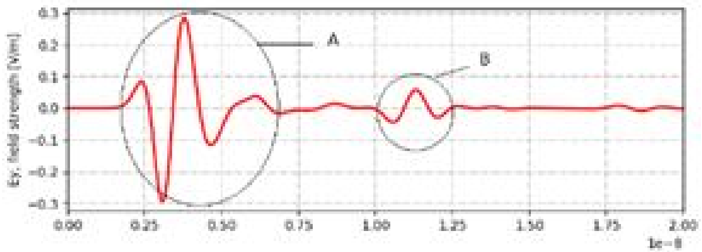

(b)

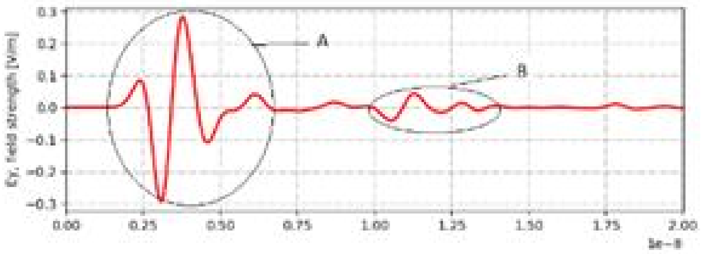

(c)

Figure 5: A-Scan Simulations Results (a) in x = 10, (b) in x = 20, (c) in x = 30.

From the results of A-Scan, in Figure 5a that is the first A-Scan scenario. For the x-axis shows time in second, while on the y-axis shows the value of voltage in Volt. Point "A" indicates the wave reflection that indicates from concrete, then the point "B" indicates the reflection of voids. Waves between points "A" and "B" are electromagnetic waves that enter the concrete before they reach voids. The reflection wave of voids is smaller than the reflection of concrete surface due to the attenuation of media being tested, and is caused by the dielectric characteristic value of voids and concrete, where the characteristic value of the voids dielectric has a smaller value so that it affects value of the voltage produced. The voltage generated at the voids reflection is around 0.05 Volts and time required to get reflection is around 0.1125 ns.

On second scenario in Figure 5b, the results of the A-Scan are seen the electric field on the y-axis because according to Fig. 3 the y-axis electric field indicates the part where the electromagnetic waves are reflected back. The voltage generated at the voids bounce is around 0.07 Volts and time required to get reflection is around 0.15 ns.

In third scenario simulation in Figure 5c, the reflection wave of voids is smaller than the reflection of concrete surface due to the attenuation of media being tested, and is caused by the dielectric characteristic value of voids and concrete, where the characteristic value of the voids dielectric has a smaller value so that it affects value of the voltage produced. The voltage generated at the voids reflection is around 0.05 Volts and time required to get reflection is around 0.1125 ns, and the results and analysis of the A-Scan simulation are explained in the Table 5.

Table 5: Analysis Results of A-Scan.

Scenario	Position of objects	Analysis results
1	10 cm, 15 cm, 50 cm (x, y, z)	Voltage = 0,05 V Time required = 0,1125 ns
2	20 cm, 15 cm, 50 cm (x, y, z)	Voltage = 0,07 V Time required = 0,15 ns
3	30 cm, 15 cm, 50 cm (x, y, z)	Voltage = 0,05 V Time required = 0,1125 ns

5.2B-Scan Signal Simulation

The first scenario is that GPR detects one object. While the object or object to be measured in the form of a ball that has the characteristics of a vacuum (air).

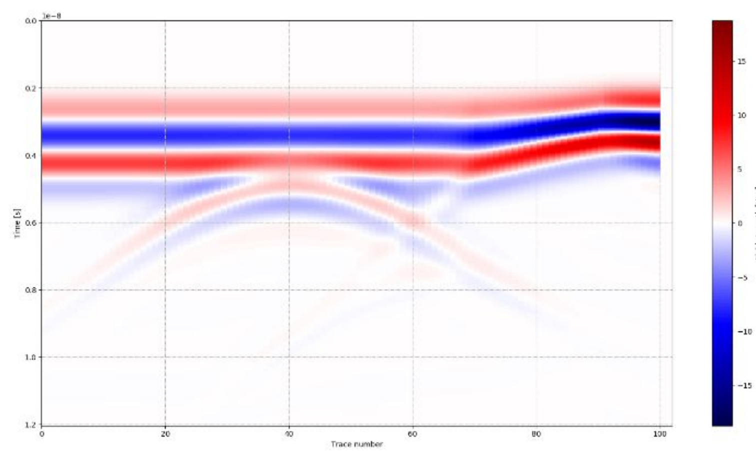

Figure 6: B-Scan 1 Object Detected.

In Figure 6, objects were detected at 4.5 ns, using the formula (1) the depth of the object is 0.257 (y-axis). And the position of the object is at 60 (x-axis), obtained from the top of the first object in the 40th sample + 10 (*Tx* antenna placement is not at position 0 but position is 10) + 10 (the difference between the *Rx* and *Tx* antennas divided by 2 or the midpoint between the *Tx* and *Rx* antennas).

The second scenario is that GPR detects two objects where the two objects are close together, they do not have enough distance. While the object or object to be measured in the form of a ball that has the characteristics of a vacuum (air).

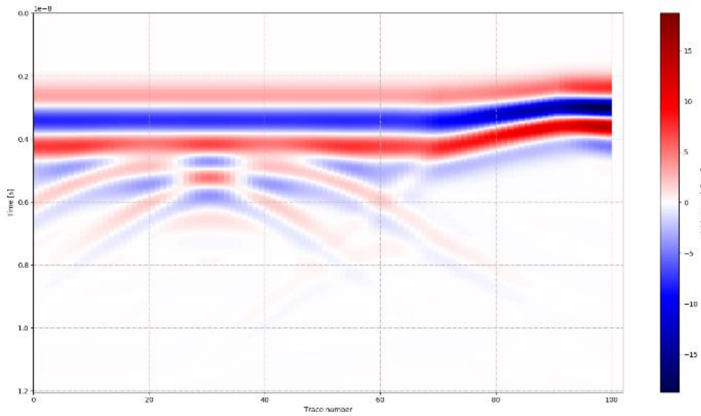

Figure 7: B-Scan 2 Objects Detected Placed Quite Close With the Distance Less Than Radar Solution.

Based on Figure 7 objects detected at 4.5 ns, using the formula (1) the depth of the object is 0.257 (y-axis), the object should be detected as many as two objects but according to Figure 7, objects detected are only one because the coordinates of objects one and objects two close together so that only one object is detected.

The third scenario is that GPR detects two objects where the two objects have a considerable distance. While the object or object to be measured in the form of a ball that has the characteristics of a vacuum (air).

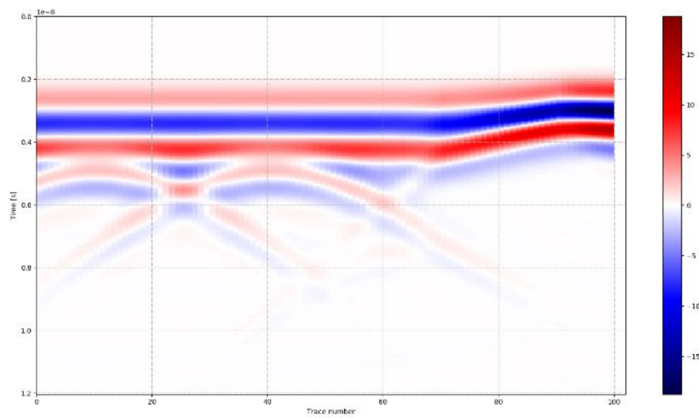

Figure 8: B-Scan 2 Objects Detected Placed With the Distance Greater Than Radar Solution.

Figure 8 explains there are two objects detected, both objects were detected at 4.5 ns, using the formula (1) the depth of both objects is 0.257 (y-axis). As well as the position of the first object at 30 (x-axis), obtained from the peak of the first object in the 10th sample + 10 (*Tx* antenna placement is not at position 0 but position is 10) + 10 (the difference between the *Rx* and *Tx* antennas divided by 2 or the midpoint between the *Tx* and *Rx* antennas), while the second object is at 60 (x-axis), obtained from the top of the first object in the 40th sample + 10 (placement of *Tx* antenna is not in 0 but position is 10) + 10 (the difference between the *Rx* and *Tx* antennas divided by 2 or the midpoint between the *Tx* and *Rx* antennas), and the results and analysis of the B-Scan simulation are explained in the Table 6.

Table 6: Analysis Results of B-Scan.

Scenario	Setting positions of object	Object position of simulation results	Time reflection of objects (simulation results)	Depth of objectuse formula (1)	Time of object was reflected (should be)
1	60 cm (x)	60 cm (x)	2,5 ns	0.257 m (y)	2,45 ns
2	40 cm (x)	Only one object detected	2,5 ns	0.257 m (y)	2,45 ns
	60 cm (x)	Only one object detected	2,5 ns	0.257 m (y)	2,45 ns
3	30 cm (x)	30 cm (x)	2,5 ns	0.257 m (y)	2,45 ns
	60 cm (x)	60 cm (x)	2,5 ns	0.257 m (y)	2,45 ns

6. CONCLUSION

In the simulation, the A-Scan signal is obtained three times by changing the position (x-axis) of the object. The position of the object's detected coordinates right in the middle between the coordinates of the antenna Tx and Rx produces a greater voltage than the object by laying the coordinates right under one of the Tx or Rx antennas. The coordinates of the detected object are right in the middle of the antenna coordinate, which takes longer than the object with the laying of the coordinates directly below one of the Tx or Rx antennas.

As for the results of the B-Scan signal output, the depth (of the y-axis) of the three B-Scan output signal experiments with depth accuracy according to the time of the object's reflection was 94.11%, for the accuracy of the object's position (towards the x-axis) for scenarios 1 and 3 100%.

REFERENCES

[1] Y. S. Kandi, R. Ramang, and R. Cornelis, "**Substitusi Agregat Halus Beton Menggunakan Kapur Alam Dan Menggunakan Pasir Laut Pada Campuran Beton (Studi Analisis Bahan Kapur Alam dan Pasir Laut Dari Kabupaten Sumba Barat Daya**

Provinsi NusaTenggara Timur)," *J. Tek. Sipil FST Undana* , vol. 1, no. 4, pp. 74–86, 2012.

[2] J. Lu, N. Xu, and S. Qu, "**Supersonic inspection of concrete using radial basis function neural network**," in *2011 International Conference on Electric Technology and Civil Engineering, ICETCE 2011 - Proceedings*, 2011, pp. 6252–6255.

[3] E. Ali, A. A. Pramudita, and D. Arseno, "**Concrete Thickness Measurement Model for GPR**," *IEEE*, no. 2, pp. 125–128, 2019.

[4] Helmi Diana, "**Investigasi Struktur Bawah Permukaan Di Lereng Gunung Raung Dengan Menggunakan Metode GPR (Ground Penetrating Radar)**," Digital Repository Universitas Jember, 2016.

[5] S. Sukode, I. J. Volume, S. Sukode, P. S. Gite, and H. Agrawal, "**Electromagnetic Interference in the Railway Spot Communication Systems**," *Int. J. Adv. Trends Comput. Sci. Eng.*, vol. 4, no. 1, pp. 1–9, 2020.

[6] C. S. Bristow and H. M. Jol, "**An introduction to ground penetrating radar (GPR) in sediments**," *Geol. Soc. London, Spec. Publ.*, vol. 211, no. 1, pp. 1–7, 2008.

[7] A. Yarovoy *et al.*, ***Ground Penetrating Radar Theory & Application***, First Edit. Oxford, UK, 2009.

[8] P. Koyan, J. Tronicke, N. Allroggen, and A. Kathage, "**Estimating moisture changes in concrete using GPR velocity analysis : potential and limitations**," *2018 17th IEEE Int. Conf. Gr. Penetrating Radar*, pp. 1–6, 2018.

[9] K. P. Rani and M. P. Reddy, "**of Advanced Trends A Comparative Study of Navigation Techniques and Information**," vol. 8, no. 1, pp. 10–14, 2019.

[10] M. A. K. Amiruddin Ab Aziz, Abdul Rahim Zulkefli, "**Finite Different Method and Differential Quadrature Method for Solving Burgers Equation**," *Int. J. Adv. Trends Comput. Sci. Eng.*, vol. 8, no. 3, pp. 10–13, 2019.

[11] A. Aziz, A. Bangert, A. G. P. R. Ground, and P. Radar, "**Model Simulation of Ground Penetrating Radar using GPRMax to Detect Porang Tuber**," *2018 17th IEEE Int. Conf. Gr. Penetrating Radar*, no. m, pp. 136–141, 2018.

[12] N. H. Shabrina, H. Nusantara, and A. Munir, "**Penggunaan Metode FDTD untuk Analisis Gelombang pada Struktur Berbasis Kartesian dan Silinder**," *JNTETI*, vol. 7, no. 3, pp. 324–330, 2018.

[13] P. Shangguan and I. L. Al-Qadi, "**Calibration of FDTD simulation of GPR signal for asphalt pavement compaction monitoring**," *IEEE Trans. Geosci. Remote Sens.*, vol. 53, no. 3, pp. 1538–1548, 2015.